applied sciences

MDPI

Article

Natural Gas Enrichment Processes and Differential Accumulation Models in the Central Anticline Belt of the Xihu Sag, East China Sea Shelf Basin

Yinshan Chang [1,*], Yiming Jiang [1], Jun Qin [1], Wenqi Chang [1], Zhiwu Xiong [1], Fujia Ji [1], Ruoyu Zhang [1] and Zhiwei Zeng [2]

[1] Shanghai Branch of the China National Offshore Oil Corporation, Shanghai 200335, China
[2] School of Geophysics and Geomatics, China University of Geosciences, Wuhan 430074, China
* Correspondence: changysh2@cnooc.com.cn

Abstract: The Central Anticline Belt of the Xihu Sag is one of the structural units with the most abundant natural gas in the East China Sea Shelf Basin. However, there are significant differences among the anticline units in terms of the scale of natural gas enrichment, occurrence horizons, types of gas reservoirs, accumulation processes, and gas-bearing properties of different strata, which influence the optimization of exploration zones and the orientation of exploration in deep-buried areas. This study conducted a comprehensive analysis in terms of the structural evolution, fault activity, hydrocarbon charging stages, and process of hydrocarbon accumulation. It clarifies that (1) the preservation condition is one of the core factors for the differential enrichment of natural gas in the Central Anticline Belt. Under the background of differential compression of the Longjing Movement, late-stage and E-W-trending faults are commonly developed in the anticline cores of the strong compression area in the south, which damage the effectiveness of traps, resulting in a large amount of natural gas escaping and being locally adjusted and accumulated in shallow effective traps. The gas reservoirs show the characteristics of multiple accumulation horizons and a small scale. In the moderately strong compression area in the north, the E-W-trending faults have weak activities and shallow incision horizons. The original gas reservoirs are not damaged, and the structures are fully filled. (2) The coupling between faults and sand bodies determines the degree of oil and gas enrichment. In the weakly compressed area in the west, late-stage E-W-trending faults are not developed, and the preservation conditions are good. The main controlled faults on the flanks of the anticline are highly active, and the coupling degree between faults and sand bodies is good, resulting in a high gas saturation. However, the transport capacity in the anticline cores is relatively poor, with a low gas saturation. (3) The differences in the paleo-structural characteristics affect the degree of oil and gas enrichment. The paleo-structures formed before the Longjing Movement provided favorable conditions for the early convergence of oil and gas. Natural gas has the characteristics of multi-stage charging, and the deep gas reservoirs have higher gas saturation than the shallow ones. On this basis, this study proposed two natural gas accumulation processes developed in the Central Anticline Belt of the Xihu Sag under the background of differential compression. One is where the hydrocarbon convergence occurs first and then oil and gas transport and accumulate into the reservoirs; the other one is where the hydrocarbon convergence and accumulation occur simultaneously, followed by gas adjustment. This paper also concludes three differential accumulation models: the local enrichment and accumulation model of gas in the strongly compressed zone, the integrated enrichment and accumulation model in the medium-strongly compressed zone, and the fault–sand coupling accumulation model in the weakly compressed zone. The results of this research have great significance for the subsequent exploration, hydrocarbon enrichment style analysis, and further strategy in the deep-buried, tight to low-permeable reservoirs in ocean exploration areas.

Keywords: natural gas of ocean; enrichment processes; accumulation models; Xihu Sag; East China Sea Shelf Basin

Citation: Chang, Y.; Jiang, Y.; Qin, J.; Chang, W.; Xiong, Z.; Ji, F.; Zhang, R.; Zeng, Z. Natural Gas Enrichment Processes and Differential Accumulation Models in the Central Anticline Belt of the Xihu Sag, East China Sea Shelf Basin. *Appl. Sci.* **2024**, *14*, 10242. https://doi.org/10.3390/app142210242

Academic Editor: Ricardo Castedo

Received: 15 October 2024
Revised: 2 November 2024
Accepted: 5 November 2024
Published: 7 November 2024

1. Introduction

The Xihu Sag of the East China Sea Shelf Basin has undergone more than 40 years of exploration [1], and several large- and medium-scale oil and gas fields have been discovered. It is the most important exploration zone and main oil and gas production area in the offshore basins of China. In recent years, a series of important exploration breakthroughs have been made in the Xihu Sag, especially in the lithologic and stratigraphic exploration fields on the flanks of the Central Anticline Belt and the deep-buried low-permeability to ultra-low-permeability fields, where large-scale natural gas exploration discoveries have been made, showing great potential for oil and gas exploration.

Series of research have been conducted on the gas migration and accumulation in the central anticline belt of the Xihu Sag, covering aspects such as source rocks, reservoirs, petrophysical properties, preservation conditions, and fault activities [2–8]. Source rocks serve as the basis for gas formation, and the gas exhibits the typical characteristic of "near-source accumulation". The closer to the effective source rock, the more favorable for hydrocarbon migration and accumulation [9–11]. The distribution and petrophysical properties of reservoirs govern the location and saturation of hydrocarbons [12–14]. Faults are generally regarded as the main migration pathways for hydrocarbons. Different fault types under various stresses determine the effectiveness of traps and thereby control the scale of hydrocarbon enrichment [15–22]. A series of international approaches toward the fault types, activities, and models have been used in characterizing the fault belt evolution and understanding processes related to climate change in the basin, which could serve as useful methods for further analysis [8,17,19].

However, there are few studies that focus on the systematic oil and gas accumulation and enrichment patterns of the Central Anticline Belt in the Xihu Sag, and there is a lack of detailed comparative studies between different structural units. The studies on the hydrocarbon accumulation process of the Central Anticline Belt are relatively weak. The main controlling factors of differential accumulation remain to be further investigated. Thus, the major aims of this article are (1) selecting typical structures in the Xihu Sag to systematically summarize the formation of gas fields, their distributions, and hydrocarbon enrichment patterns, (2) combining various information such as structural evolution, fault conductivity, and geochemical characteristics to comparatively analyze the gas accumulation process in different structural units and conclude the main factors controlling the differential accumulation, and (3) discussing and establishing the gas accumulation models of different structural units of the Central Anticline Belt in the Xihu Sag, East China Sea Shelf Basin.

2. Geological Setting

The Central Anticline Belt is located in the middle of the Xihu Sag, bordered by the western slope zone to the west and the Diaoyudao Uplift to the east (Figure 1a), develops a series of anticlines, and is located in the hydrocarbon-generating sub-sag. It was formed in the Longjing Movement at approximately 13 Ma, and is one of the most favorable areas for gas accumulation. The Xihu Sag has undergone several tectonic events: the Paleocene–Eocene syn-rift stage, the Oligocene–Miocene early post-rift stage, and the Pliocene–present late post-rift stage (regional subsidence) [23,24]. Among them, the Longjing Movement since the Miocene has had the most significant impact on the formation and evolution of the Central Anticline Belt, as well as on oil and gas accumulation. The E-W compressional stress during the Longjing Movement led to the formation of this NE-SW-oriented Central Anticline Belt and caused the strata in the Central Anticline Belt to be significantly uplifted and eroded [25–27].

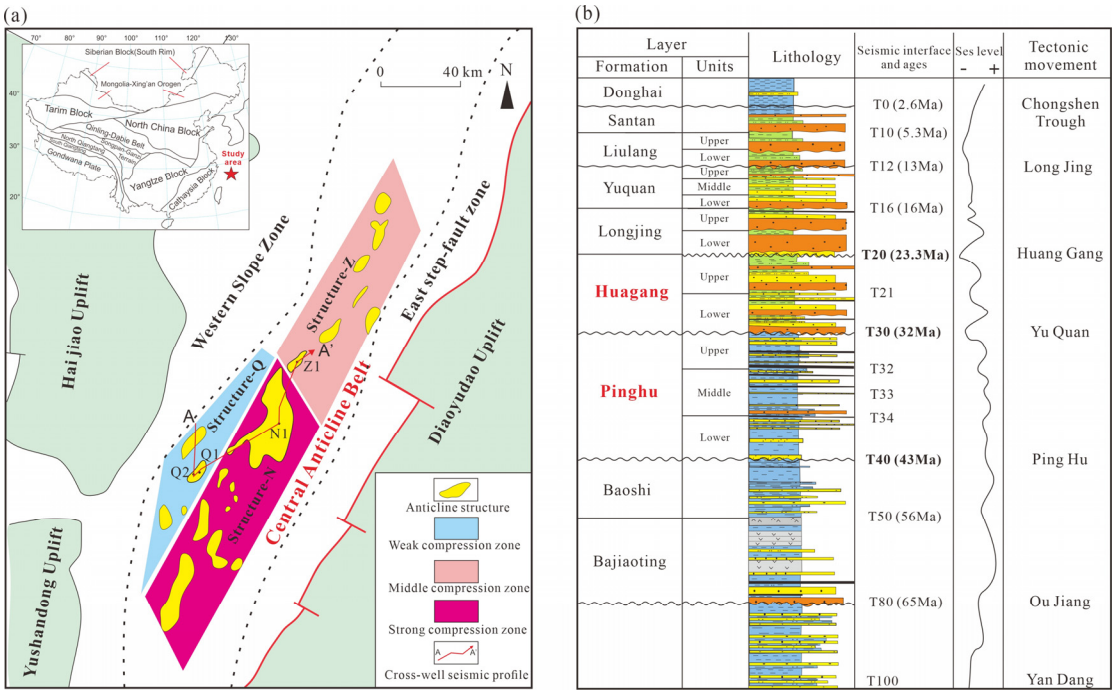

Figure 1. (**a**) Regional geological maps of the Central Anticline Belt in the Xihu Sag in the East China Sea Shelf Basin, including the major anticline structures, various compression zones, cross-well seismic profile A–A′, and drilled wells used in this study. (**b**) Stratigraphic map of the Xihu Sag, showing the lithology, sea-level curve, seismic interfaces and ages, formation, and tectonic movement.

The Xihu Sag deposits a series of Cenozoic strata (Figure 1b): from bottom to top, this includes the Eocene Pinghu Formation (T40–T30), the Oligocene Huagang Formation (T30–T20), the Miocene Longjing Formation (T20–T16), Yuquan Formation (T16–T12), Liulang Formation (T12–T10), the Pliocene Santan Formation (T10–T0), and the Quaternary Donghai Formation. It is worth noting that the Eocene–Oligocene Pinghu Formation and Huagang Formation are the study intervals of this research. The Pinghu Formation was formed during the syn-rift stage, depositing shallow marine to continental sediments [28,29]. It contains significant source rocks and reservoirs and is a hydrocarbon-bearing formation in the Xihu Sag. The Huagang Formation mainly developed during the early post-rift stage of the basin, depositing a typical set of fluvial–lacustrine strata with a thickness of 600 m to 1000 m. It is also one of the main target layers for oil and gas exploration in the Xihu Sag.

3. Dataset and Methods

This study mainly utilizes the drilled-well data of four wells, namely Q1, Q2, N1, and Z1 from structures Q and N (Figure 1a), as well as the analysis and testing data of 35 core samples related to these four wells. The completed test analyses in this study mainly include scanning electron microscope (SEM) analysis, carbon isotope ($\delta^{13}C_1$) analysis, and fluid inclusion analysis, etc. Among them, the SEM analysis was completed at the Jiangsu Oilfield Experiment Center. The illite K-Ar dating shows that the oil and gas charging time was 25.14 Ma. Meanwhile, the Central Anticline Belt structural area is covered by high-resolution 3D seismic data, which were collected in 2018, with an area of approximately 300 km^2. They were collected by dual-vessel, three-dimensional, and ten-streamer acquisition, with a coverage of 54 times and a cable spacing of 75 m. In addition, the location of cross-well seismic profile A–A′ used in this study is shown in Figure 1.

This paper summarizes the development and enrichment characteristics of natural gas reservoirs in different structures of the Central Anticline Belt through a comprehensive research method of drilling-wells data and 3D seismic data. Combining the evolution

characteristics of different structures of the Central Anticline Belt, integrated with the analysis of oil and gas transport capacity of faults and the geochemical characteristics of oil and gas in this study, we try to compare the oil and gas accumulation process of various structures (Q, N, Z) and propose different natural gas accumulation models of the Central Anticline Belt.

4. Result and Interpretation

4.1. Differential Enrichment Characteristics of Various Anticline Structures

According to the intensity of the compressive stress and the scale of the anticline, the Central Anticline Belt in this research can be divided into three different structures, including a northern medium-strong compression zone (Structure-Z), a southern strong compression zone (Structure-N), and a western weak compression zone (Structure-Q; Figure 2). Due to different structural evolution processes, preservation conditions, hydrocarbon migration and accumulation processes, etc., the gas enrichment characteristics of each anticline structures show differences in the gas column, gas filling degree, and reserve abundance (Figure 3).

Structure-Z is fully saturated and located in the northern medium-strong compressed zone of the northern Central Anticline Belt (Figure 1a), covering an area of 40 km^2. It is an inversion anticline formed during the Longjing Movement, with an amplitude of approximately 400 m. The hydrocarbon-bearing strata (H1–H7) are located below the regional mud-seal H1–H2 in the Huagang Formation (Figure 3). The gas column of Structure-Z is 400 m, with a 100% gas filling degree and 12.4 m^3/km^2 reserve abundance (Figure 2).

Structure-N is located in the southern strongly compressed zone of the Central Anticline Belt (Figure 1a), with an anticline area of 700 km^2 and an anticline amplitude of approximately 850 m. It is the largest anticline in the offshore areas of China. Hydrocarbons have been encountered in multiple horizons vertically, ranging from the Huagang Formation to the Longjing Formation (Figure 3). However, the gas column is generally less than 50 m, and most of the gas reservoirs are underlain by water. The proportion of the volume filled by hydrocarbons in this anticline is less than 20%, with 2.5 m^3/km^2 reserve abundance (Figure 2).

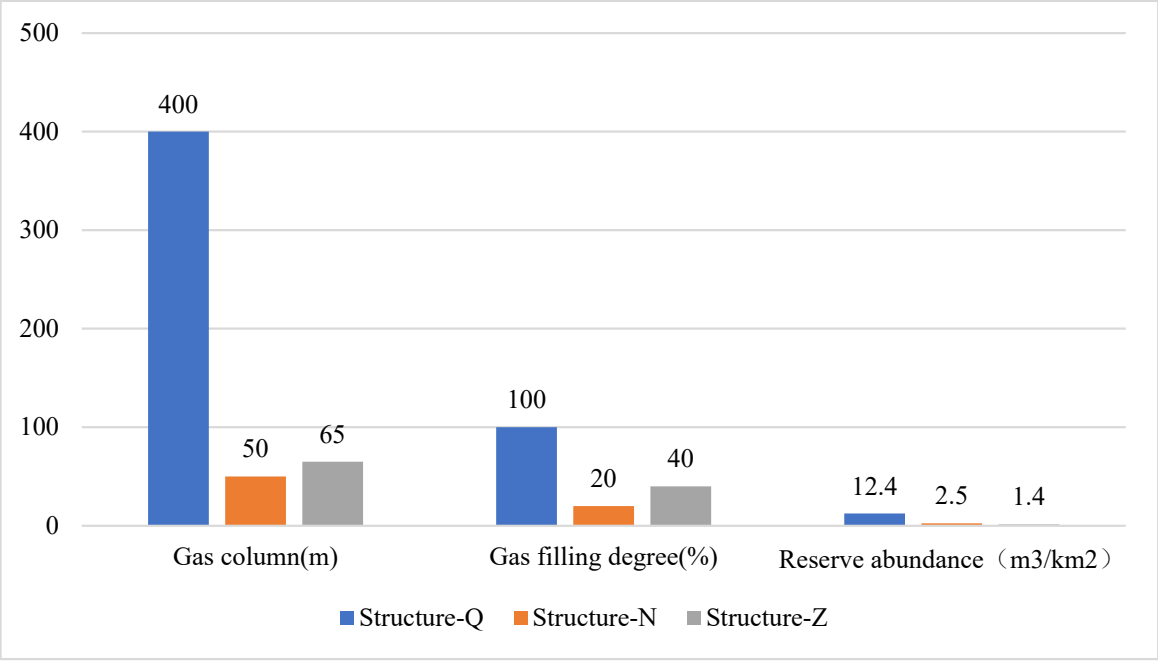

Figure 2. Differential enrichment characteristics of natural gas in the anticline structure Q, N, and Z of the Central Anticline Belt.

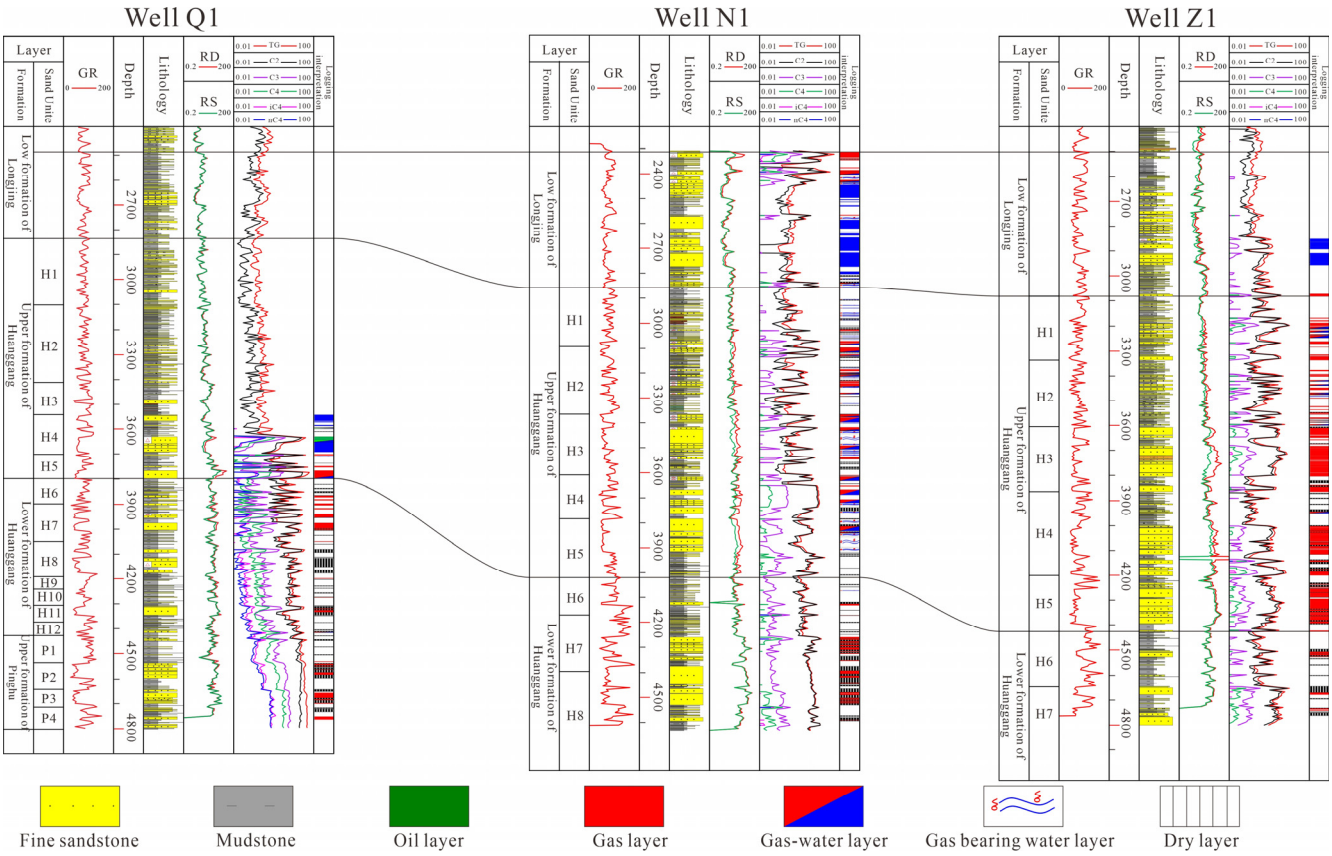

Figure 3. Three single-well diagrams for three different structures (Q, N, and Z) in the Central Anticline Zone, including gamma ray (GR) curves, lithological association, deep and shallow lateral resistivity (RD, RS) curves, and logging interpretation of oil, gas, and water layers. The location of the three wells is shown in Figure 1a.

Structure-Q is located in the western weakly compressed zone of the Central Anticline Belt (Figure 1a). It is a low-amplitude anticline structure formed under the compressive background of the Longjing Movement, with an anticline area of 60 km^2 and an amplitude of about 100 m. The main hydrocarbon reservoir strata of this structure are the H4 and deeper strata of the Huagang Formation (Figure 3). The anticline core and flank of this structure have different gas–water interfaces. The maximum height of the gas column is 65 m, the gas saturation or filling degree is 40%, and the reserve abundance is approximately 1.4 m^3/km^2 (Figure 2).

It is worth noting that thick-layer, ultra-low-permeability gas reservoirs are developed in the deep layers of these three anticline structures (Z, N, and Q), with huge reserve scales. However, there are significant differences in the gas-bearing properties of the gas reservoirs. Among them, in Structure-Z, the permeability average of Sandstone Group-5 of the Huagang Formation (H5) is 0.28 mD, and the average gas saturation is 53%. In Structure-N, the permeability average of Sandstone Group-7 of the Huagang Formation (H7) is 0.25 mD, and the average gas saturation is only 42%. In Structure-Q, the permeability average of Sandstone Group-2 of the Pinghu Formation (P2) is 0.38 mD, and the average gas saturation is 48%.

4.2. Natural Gas Preservation Condition of the Central Anticline Belt

Sandstone Group-1 and Group-2 of the Huagang Formation (H1–H2) sand–mudstone-interbedded units in the Central Anticline Belt of the Xihu Sag are the most stable regional mudstone caprock, with a thickness of approximately 600 m, mainly consisting of micro-facies of flood plains in the delta plain. This set of regional caprocks is mainly composed

of thick mudstone intercalated with thin siltstone, with a high argillaceous content and a mud-to-land ratio of approximately 60%. Most of the oil- and gas-bearing strata in the Central Anticline Belt are located beneath this set of regional caprocks (Figure 4). However, under the background of strong compression during the Longjing Movement, a series of late-stage EW-trending fault systems are commonly developed in the anticline cores of the northern medium-strong compression zone (Structure-Z) and the southern strong compression zone (Structure-N) (Figure 4). Their planar distribution scale is relatively small. Vertically, these faults can extend downward through the regional mudstone caprock and cut into the main oil- and gas-bearing strata, such as H3 and H5, and, upward, they can reach the T10 interface at the top of the Miocene strata. The late-stage fault activities have significant adjustment, transformation, and destructive effects on the natural gas reservoirs of the Huagang Formation, resulting in the large-scale escape of natural gas and local adjustment and accumulation in the effective traps of the shallow Longjing Formation.

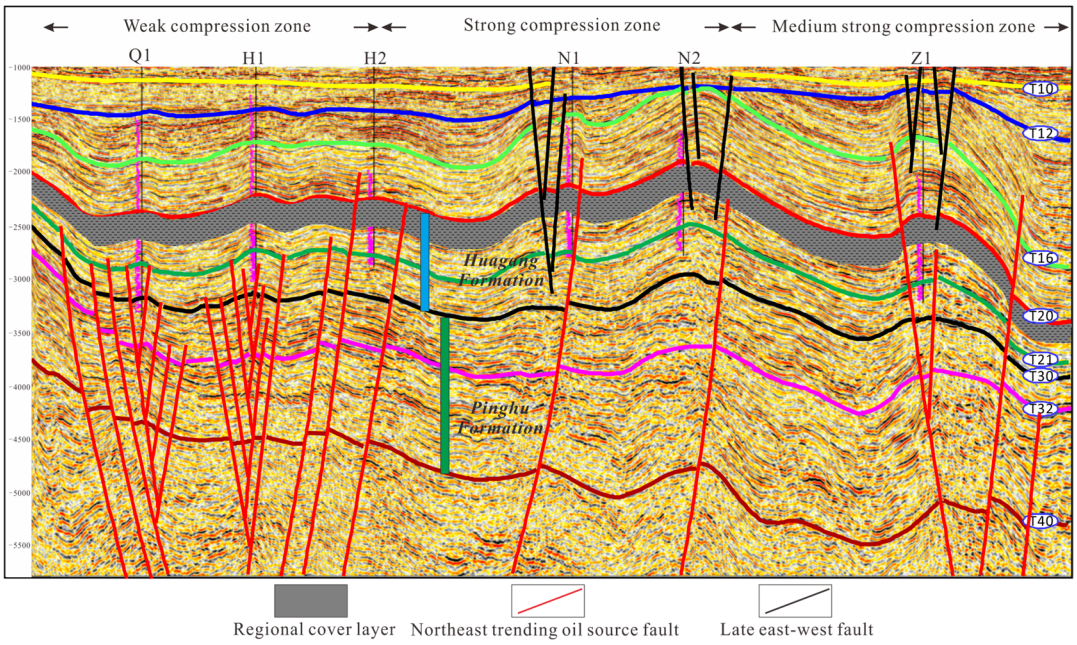

Figure 4. Seismic profile A–A′ of different compression zones of the Central Anticline Belt, showing the features of regional cap rock, and NE-trending and EW-trending fault systems developed in various structures. The location of the seismic profile A–A′ is shown in Figure 1a.

In the southern strongly compressed zone, under the intense compression background of the Longjing Movement, Structure-N has generally developed near E-W trending transverse tensile destructive faults in its anticline core, which have damaged the original gas reservoirs of the deep H3–H5 sand groups. Natural gas has been adjusted and accumulated in the effective traps of the shallow Longjing Formation. This has led to multiple oil- and gas-bearing strata in the vertical direction in this structural area, with small gas reservoir scales and common water presence. For instance, in well-N1, the current H3 is a bottom water gas reservoir with a gas layer thickness of approximately 8.4 m (Figure 5). The LINKAM THMS600-type heating and cooling stage of the nuclear industry was used to conduct gains containing oil inclusions (GOI) analysis and quantitative grain fluorescence analysis for the gas–water layer and the entire water layer section of the H3b gas layer in well-N1. Generally, it is considered that a hydrocarbon-bearing inclusion GOI $\geq$ 5% and QGF-index $\geq$ 4 are the basis for paleo-oil and gas reservoirs [30–34]. It can be seen that the GOI of hydrocarbon-bearing inclusions in H3 of well-N1 is <5% at 3198 m, and 3155 m is taken as the paleo gas–water interface. Through the analysis of the paleo-oil and gas reservoir interface, the thickness of the paleo gas layer of H3b is 72 m, indicating that H3 of Structure-N was a damaged residual gas reservoir of the Huagang Formation. Under

the destructive effect of the late near-E-W-trending faults, a large amount of natural gas escaped into the shallow Longjing Formation.

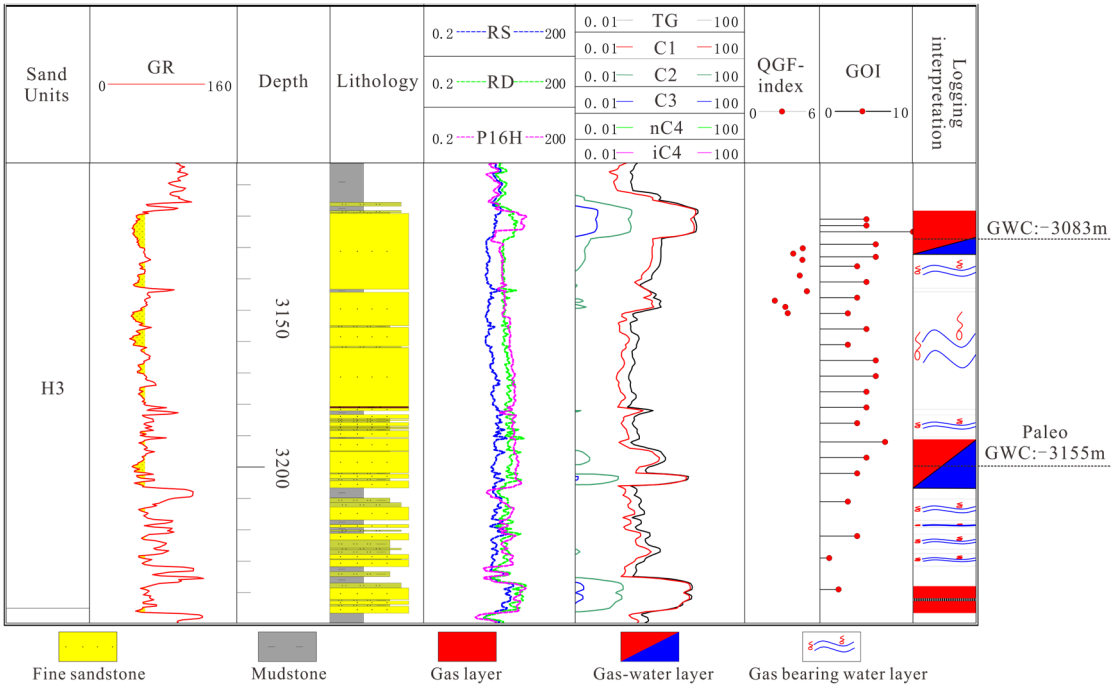

Figure 5. The well-N1 composite bar chart of the H3 sand group of the Huagang Formation, including the gamma ray (GR) curves, lithology, various logging curves, QGF-index data, gains containing oil inclusions (GOI) data, and gas–water contact (GWC) logging interpretation.

In the northern medium-strong compression zone, the anticline core of Structure-Z also developed late-stage near-EW-trending transverse tensile faults, but its compression degree was relatively weak. The faults converged downward in the H1-H2 regional mudstone caprock and did not damage the main gas-bearing strata such as the H3 sand group in the Huagang Formation. Therefore, the gas reservoir preservation conditions of Structure-Z were better, and the anticline structure was fully filled with natural gas.

4.3. Fault Activity and Coupling Degree of Fault–Sand Body

Hydrocarbon migration is one of the key elements for hydrocarbon accumulation systems outside the oil source [35]. The late-stage activities of the NE-trending oil-source faults in the northern medium-strong compression zone (Structure-Z) and the southern strong compression zone (Structure-N) of the Central Anticline Belt are strong, and they can extend upward to the T16 interface. The coupling degree between the faults and the sand bodies is high, and they have a strong hydrocarbon migration and charging capacity. In comparison, Structure-Q located in the western weakly compressed zone of the Central Anticline Belt has relatively weak late-stage tectonic activities and no late-stage faults, and the preservation conditions of the oil reservoir are good. However, the NE-trending oil-source faults of Structure-Q have weak activities, and the faults only extend upward to the T21 interface, and its main reservoir-forming strata are all located in the strata deeper than H4 of the Huagang Formation.

Structure-Q has the characteristics of a flower-like structure (Figure 6). Its third-level main control faults develop on the flank of the anticline, with relatively large-scale and strong fault activity. The oil-source faults can extend upward to the T21 interface and downward to the T40 interface, with a strong hydrocarbon migration and conduction capacity. The anticline core of this structure Q is mainly composed of fourth-level adjustment faults, which have a smaller fault scale and limited cut-through horizons (Figure 6). Therefore, the hydrocarbon migration capacity of the fourth-level faults is also relatively limited. Well-Q1

is located in the core of anticline Structure-Q, and the migration fault is a fourth-level adjustment fault. The gas column of the main layer H5 is 25 m, and the inclusion abundance is less than 5%, indicating that there is no large-scale hydrocarbon charging and that the hydrocarbon migration capacity is limited. In contrast, well-Q2 is located on the west flank of the anticline Structure-Q, and the migration fault is the third-level fault F1. The coupling and matching of the fault and sand body are good, and the gas column height of the gas reservoir is 65 m. By comparing the hydrocarbon accumulation characteristics of well-Q1 in the anticline core and well-Q2 in the anticline flank, it can be determined that the oil-source faults located in the flank of the anticline structure have a higher level, stronger cut-through activity, and stronger hydrocarbon conduction capacity.

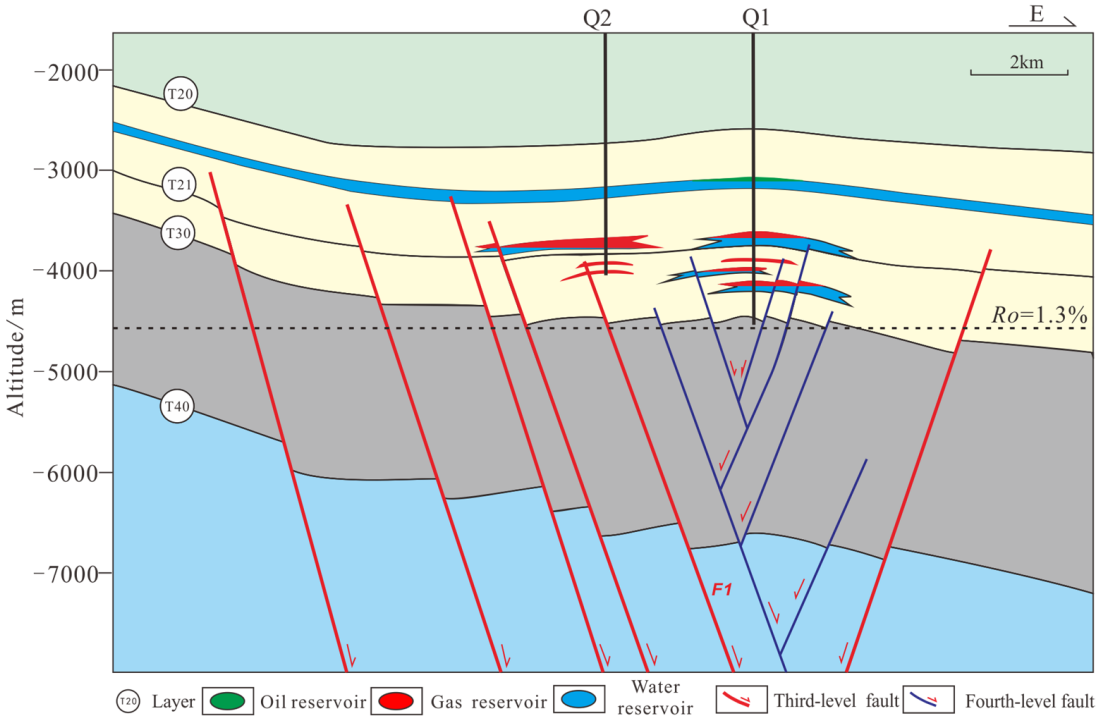

Figure 6. Typical cross-wells section of Structure-Q, showing hydrocarbon charging and the hydrocarbon migration features with various-level fault systems. The location of the two wells is shown in Figure 1a.

4.4. Paleo-Structure Characteristics of Differential Enrichment of Gas

The paleo-structural background is one of the important controlling factors for the degree of oil and gas enrichment in the Central Anticline Belt of the Xihu Sag. A large number of oil and gas exploration practices have proved that, in the dynamic process of oil and gas migration and accumulation, paleo-structures are often favorable target areas for paleo-oil and gas migration [36–39]. Meanwhile, paleo-structures provide important sites and trapping conditions for the accumulation of paleo-oil and gas, and also have an important impact on the formation and distribution of current oil and gas reservoirs. The Xihu Sag has undergone multiple tectonic movements, among which the Longjing Movement since the Miocene has the greatest influence on the formation and evolution of the Central Anticline Belt and the accumulation of oil and gas. Before the Longjing Movement, the Xihu Sag experienced a series of tectonic movements, such as the Yuquan and Huagang movements, which controlled the paleo-structural background of the early Xihu Sag.

By restoring the paleo-structure of the top surface of the source rock strata of the Pinghu Formation during the period of 16 Ma (Figure 7b), it can be seen that the paleo-structure had already formed before the large-scale charging and accumulation of natural gas, and it is quite different from the current structural map (Figure 7a). Among them, Structure-Q and Structure-Z

developed nosing paleo-structures, while Structure-N was a negative unit before the oil and gas charging and did not develop a paleo-structure during 16 Ma (Figure 7b).

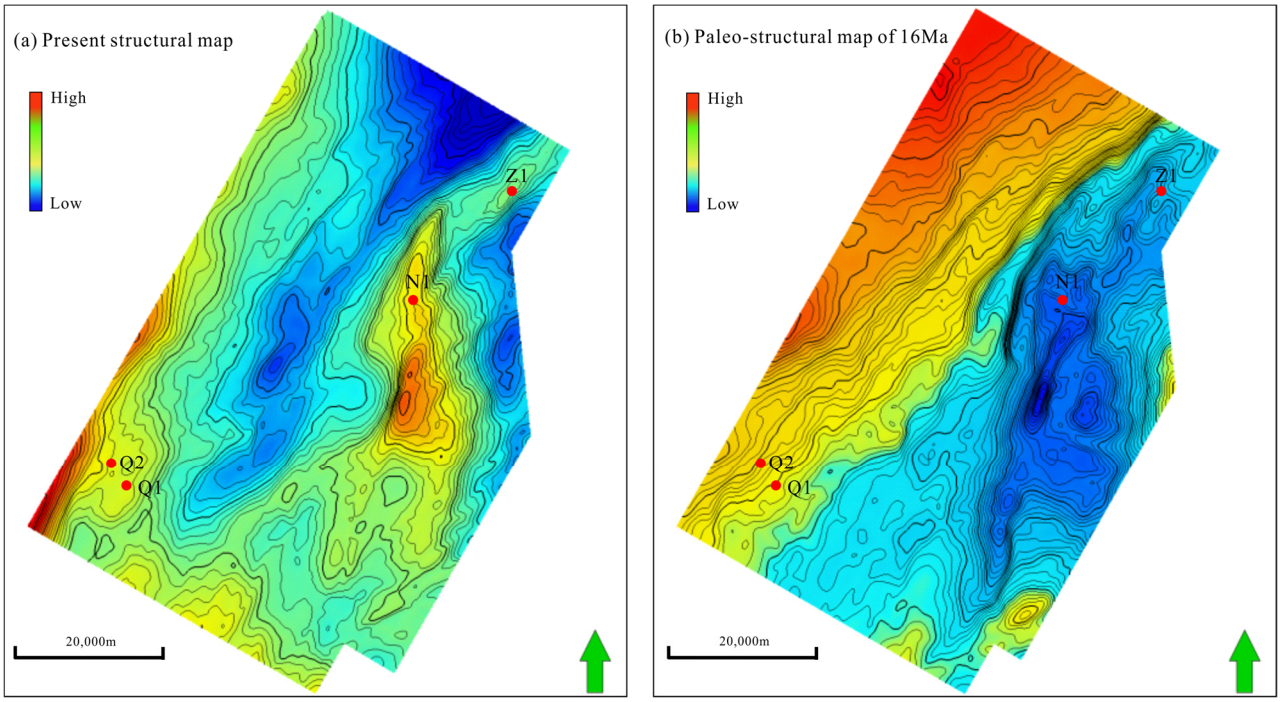

Figure 7. (**a**) The present structural map and (**b**) the paleo-structure map of top Pinghu formation at 16 Ma of the study area in the Central Anticline Belt.

The paleo-structural background of Structure-Q was formed by the compression of the Longjing Movement (Figure 7b), providing a favorable site for the early oil and gas charging or trapping. According to the analysis of the P2-layer sandstone samples from well-Q1, two stages of oil and gas inclusions were developed (Figure 8). The first stage of oil and gas inclusions developed in the early to middle stage of the secondary enlargement of quartz grains in sandstone, with a low development abundance and a GOI of about 3%. Most of the first-stage inclusions are distributed in bands along the inner side of the enlarged edge of quartz grains and along the micro-fractures during the diagenesis of quartz grains (Figure 8), and the homogenization temperature of the inclusions is 120 °C to 130 °C. The second stage of oil and gas inclusions developed after the secondary enlargement of quartz grains in sandstone, with a high development abundance and a GOI of about 15%. Most of the second-stage inclusions are distributed in bands along the post-diagenetic micro-fractures that cut through quartz grains and their enlarged edges (Figure 8), and the homogenization temperature of the inclusions is 140 °C to 150 °C. In addition, from the analysis of the methane carbon isotopes of natural gas in the Pinghu Formation and Huagang Formation of the Q structure, it is also confirmed that the Q structure has the characteristics of multi-stage charging. Vertically, from the deep Pinghu Formation to the shallow Huagang Formation, the methane carbon isotope differentiation of natural gas is relatively large, exceeding 3‰. Gradually, the methane carbon isotope is shown heavier upward, increasing from −30.7‰ to −33.8‰ (Figure 9a), reflecting the gradually increasing maturity of the source rocks and the multi-stage charging characteristics of natural gas.

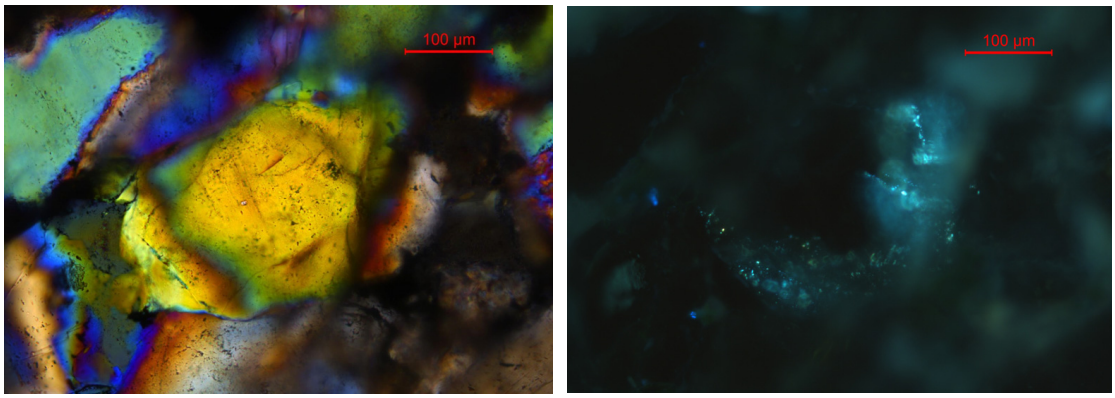

Figure 8. The hydrocarbon inclusion characteristics of sandstone sampled from P2 of well-Q1.

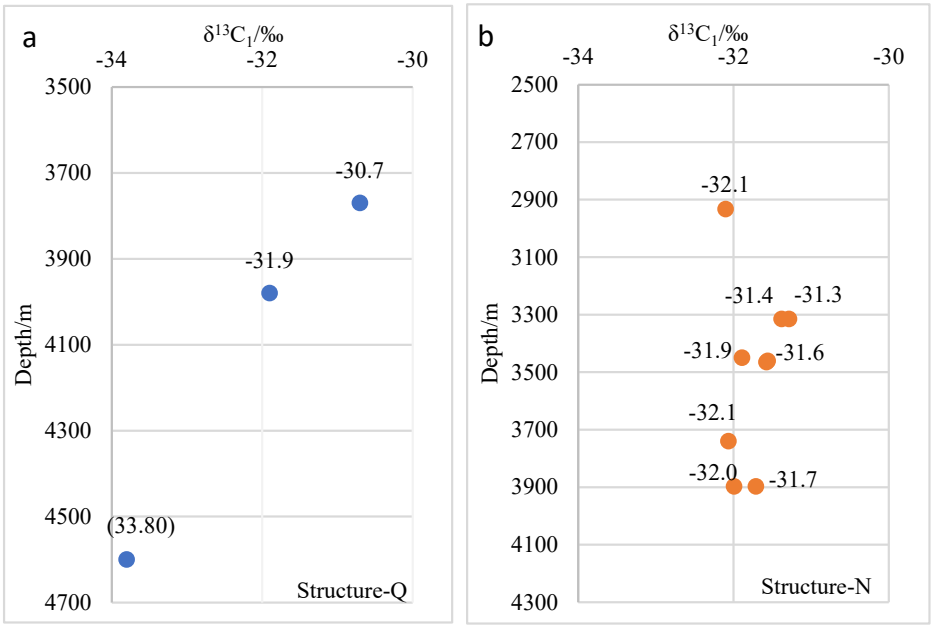

Figure 9. Methane carbon isotopes data of (**a**) Structure-Q and (**b**) Structure-N.

However, Structure-N did not develop a paleo-structure before the Longjing Movement (Figure 7b), and it was overall a sub-sag area during the paleo-structure at 16 Ma. One stage of oil and gas inclusions can be identified in the sandstone samples of well-N1 (Figure 10). The inclusions developed within the micro-fractures that cut through the early quartz grains or the late micro-fractures that cut through the enlarged edges, with a GOI of 6–12%. In addition, based on the methane carbon isotope analysis of Structure-N (Figure 9b), the methane isotope values of different strata are relatively close, ranging between −30.5 and −32.1‰, and the vast majority are around −31‰ (Figure 9b), indicating that the natural gas of this structure has the characteristics of charging in the same period. Due to the lack of the early convergence process of natural gas in Structure-N, the gas saturation of the gas layers encountered in the ultra-low permeability field is generally low.

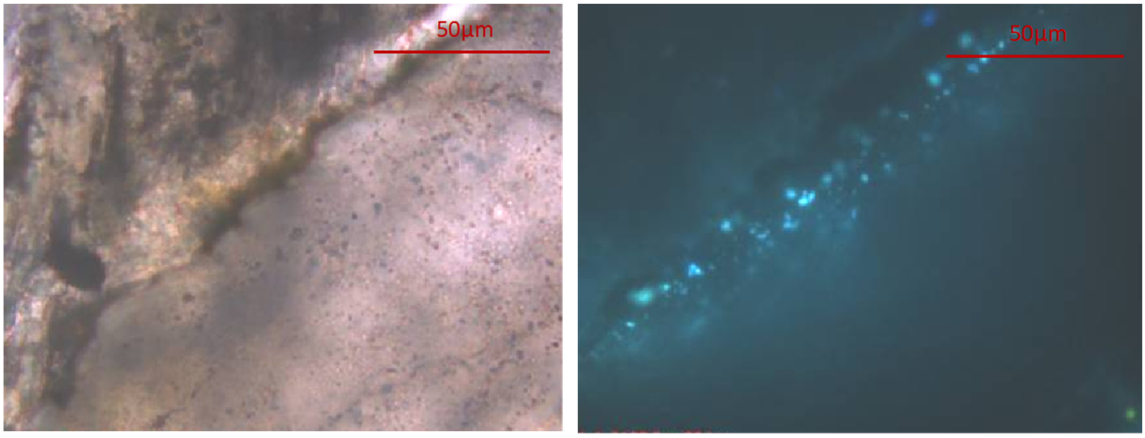

Figure 10. The hydrocarbon inclusion characteristics of sandstone sampled from Huagang Formation of well-N1.

5. Discussions

5.1. Natural Gas Enrichment Processes of the Central Anticline Belt

It is currently widely believed that the large-scale charging and accumulation of natural gas in the Central Anticline Belt of the Xihu Sag are closely related to the Longjing Movement, especially with the late accumulation at 13 Ma being the main process. By comparing the characteristics of oil and gas reservoirs of the three typical anticline structures of N, Q, and Z in the Central Anticline Belt, this study believes that there are significant differences in the natural gas accumulation processes of different anticline structures. Generally, there are two natural gas accumulation models: one is where the hydrocarbon convergence occurs first and then oil and gas transport and accumulate into the upper structural reservoirs; the other one is where the hydrocarbon migration and oil and gas accumulation occur simultaneously, followed by hydrocarbon adjustment.

(1) Model 1 of natural gas enrichment process

Model 1 is referred to as "the hydrocarbon convergence occurs first and then oil and gas transport and accumulate into the upper structural reservoirs", which is the typical pattern of the natural gas enrichment process. The main hydrocarbon-generating sub-sags in the Xihu Sag began to generate and expel hydrocarbons around 25 Ma [40]. During the hydrocarbon generation and expulsion period, the source rock strata first experienced a short-distance migration and convergence of source rocks in the pre-existing paleo-structures of the basin to form oil and gas reservoirs. When the source rock strata are in low-amplitude structures, gentle steps, or nose-like structures, hydrocarbons will also undergo migration and convergence. These accumulated or semi-accumulated hydrocarbons can further undergo vertical migration during late tectonic movements, be further transported upward, and accumulate and form reservoirs in traps. Before the Longjing Movement in Structures-Q and -Z, the source rock strata of the Pinghu Formation already had a certain paleo-structural background, so oil and gas were preferentially transported and accumulated in the direction of the paleo-structure, while the traps of the Huagang Formation were formed late and the ancient and modern structures were connected by faults, forming a "the hydrocarbon convergence occurs first and then oil and gas accumulate into the upper structural reservoirs" pattern (Figure 11). The previous text has comprehensively discussed oil and gas inclusions, natural gas methane carbon isotopes, etc., under a certain paleo-structural background, effectively confirming this natural gas enrichment process.

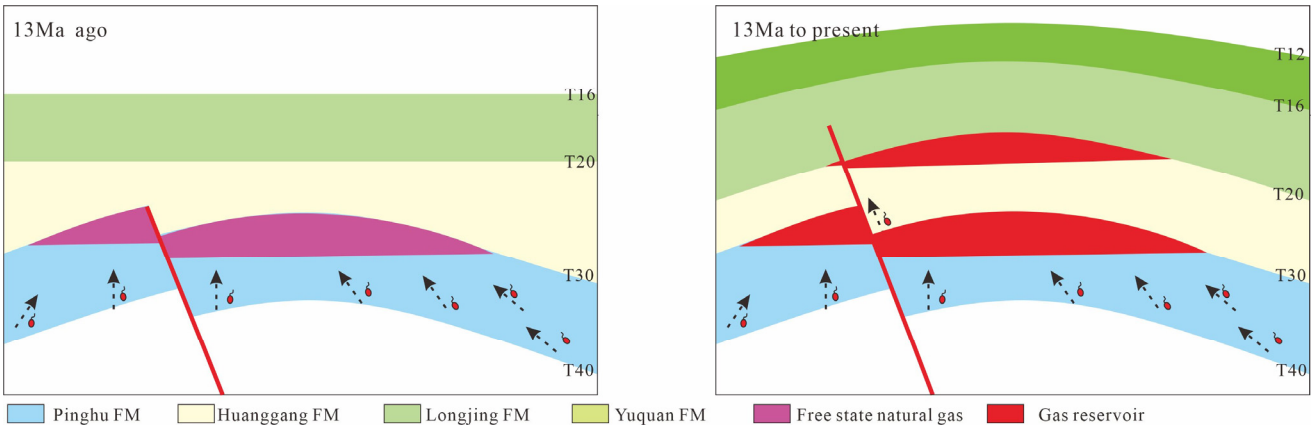

Figure 11. The natural gas enrichment process pattern of hydrocarbon convergence occurs first and then oil and gas accumulate into the upper structural reservoirs.

In the first process of natural gas enrichment, the deep gas reservoirs have the characteristics of early natural gas charging based on the pre-convergence and also have a higher gas saturation (Figure 11). By comparing the microscopic reservoir characteristics of and differences in the P2 layer and H7 layer of well-Q1 (Figure 12), although both layers belong to ultra-low-permeability reservoirs, under the background of early oil and gas convergence in the P2 layer, the formation of illite was inhibited (Figure 12d–f). Illite K-Ar dating indicates that the hydrocarbon charging time is approximately 25 Ma. Therefore, the overall pore-throat structure of the P2 layer sand body is relatively clean, and the maximum gas saturation is 52%, while the oil and gas charging of the H7 layer is related to the Longjing Movement, and the oil and gas charging time is relatively late (about 13 Ma). The maximum gas saturation of the gas reservoir in the Huagang Formation is only 45%.

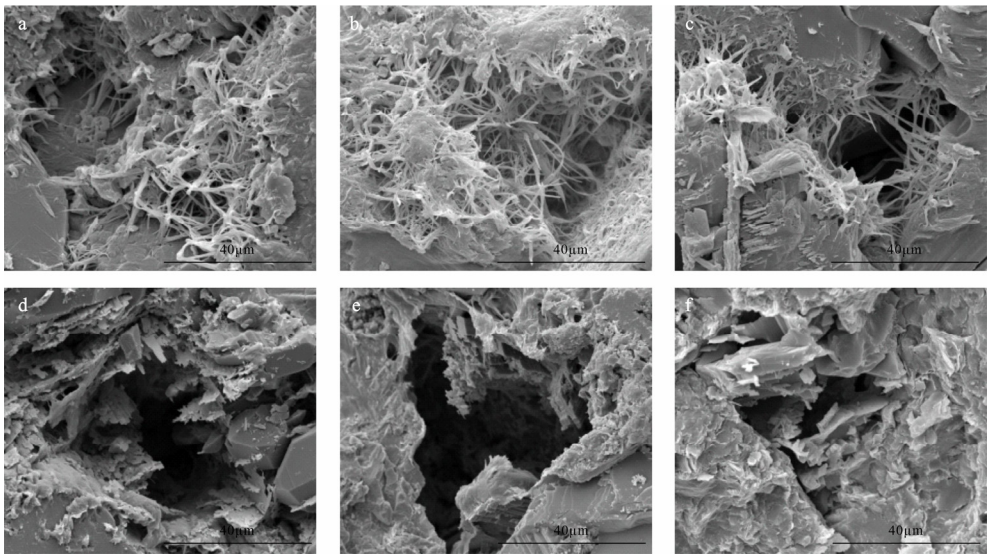

Figure 12. Comparison of scanning electron microscopy (SEM) characteristics between P2 and H7 sand groups of well-Q1. (**a**–**c**) H7, 3978.98 m, the pore throat is filled with a large amount of illite, which appears as filamentous or bridge-like structures. (**d**–**f**) P2, 4330.34 m, dissolution forms secondary intergranular enlarged pores, with a very small amount of illite distributed in the pores.

(2) Model 2 of natural gas enrichment process

Model 2 of the natural gas enrichment process is related to the fact that "The hydrocarbon migration and accumulation occur simultaneously, followed by later hydrocarbon adjustment". When the source rock strata in the Xihu Sag do not have a paleo-structural

background, oil and gas cannot undergo migration and accumulation preferentially. Under the later tectonic movement, natural gas can directly undergo vertical migration and accumulate in the high part of the structure to form a reservoir (Figure 13). Structure-N was a low-lying area before the Longjing Movement. The early oil and gas convergence area was in the surrounding areas of the sag. Under the action of the late-stage Longjing Movement, natural gas migrated and charged to the current high part of the structure and accumulated to form a reservoir. At the same time, under the background of strong compression, the EW-trending faults will damage the gas reservoir of the Huagang Formation and adjust and accumulate in the effective traps of the shallower Longjing Formation (Figure 13).

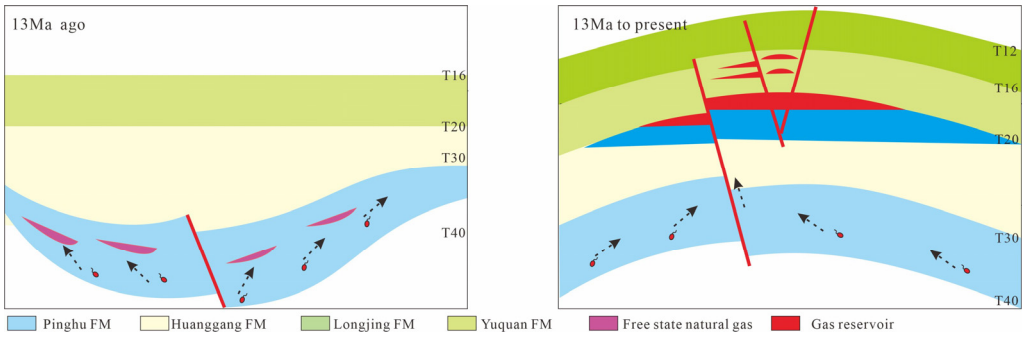

Figure 13. The natural gas enrichment process pattern of the hydrocarbon migration and accumulation occurring simultaneously, followed by later hydrocarbon adjustment under the Longjing movement.

5.2. Different Natural Gas Accumulation Models of Various Anticline Structures

By comparing the main controlling factors of natural gas enrichment processes of the three typical anticline structures (Z, N, and Q) under different compressive stress backgrounds, three different natural gas accumulation models of the Central Anticline Belt in the Xihu Sag can be established (Figure 14).

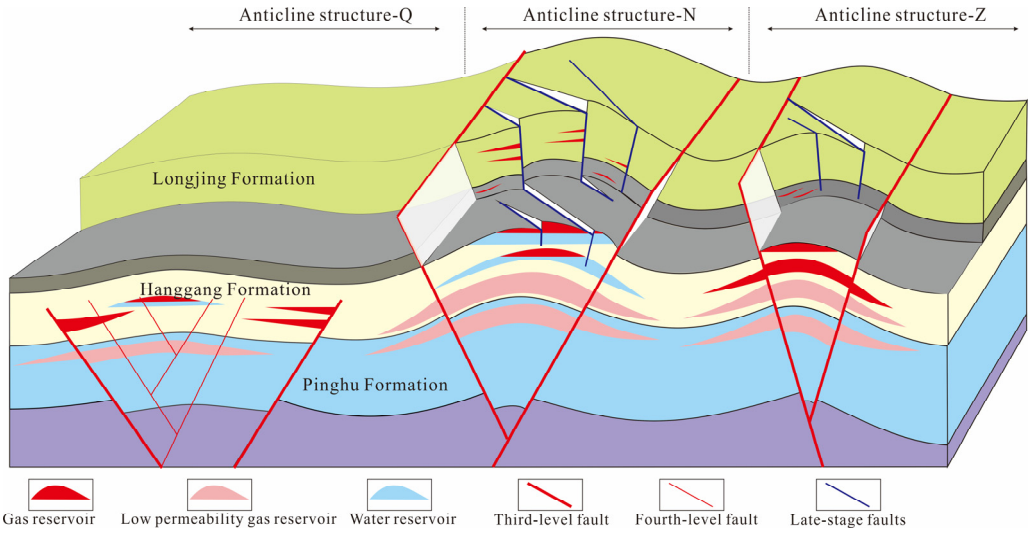

Figure 14. Differential natural gas accumulation models in different compression zones of the Central Anticline Belt in the Xihu Sag.

(1) "Integral anticline" accumulation model in the northern Medium-Strong Compression Zone (Structure-Z): The compressive intensity of the Longjing Movement was relatively moderate, and a complete anticline structure was developed. The NE-trending faults were highly active. Meanwhile, although the EW-trending faults developed in the late stage in the anticline core, they did not cut through to the main reservoir

strata. Therefore, the trap preservation conditions were good, enabling the formation of an integral large-scale gas field.

(2) "Local enrichment" accumulation model in the southern Strong Compression Zone (Structure-N): Under the strong compression background of the Longjing Movement, a series of giant anticline structures were formed, with large amplitudes of the anticlines and strong fault activities and natural gas migration. However, the late EW-trending fault systems were commonly developed in the anticline cores, generally cutting through the main reservoir strata, such as the Huagang Formation, resulting in the large-scale escape of natural gas. Only a part accumulated effectively again in the shallow Longjing Formation; thus, the gas reservoir showed the characteristics of a small-scale and scattered distribution.

(3) "Fault-sandbody coupling" accumulation model in the western Weak Compression Zone (Structure-Q): The degree of compression was relatively weak, the amplitude of the anticline was low, and no late-stage destructive faults were developed in the anticline core. Therefore, the preservation conditions of the structural traps were good. However, due to the weak activity of the oil-source faults trending northeast, the fault activity and the coupling degree with the sand body determined the enrichment degree of the gas reservoir.

6. Conclusions

The main conclusions of this study are as follows:

(1) Based on the comprehensive analysis of different characteristics of natural gas in various anticline structures in the Central Anticline Belt of the Xihu Sag, it is clarified that, under the background of differential compression of the Longjing Movement, the preservation conditions of traps, fault activity, the coupling degree of faults and sand bodies, and the paleo-structural background are the most influential factors for the differential enrichment of natural gas in the Central Anticline Belt.

(2) Two natural gas accumulation processes developed in the Central Anticline Belt of the Xihu Sag are proposed under the background of differential compression. One is where the hydrocarbon convergence occurs first and then oil and gas transport and accumulate into the reservoirs; the other one is where the hydrocarbon convergence and accumulation occur simultaneously, followed by gas adjustment. In addition, this paper also concludes three differential accumulation models: the "Integral anticline" accumulation model in the northern Medium-Strong Compression Zone, the "Local enrichment" accumulation model in the southern Strong Compression Zone, and the "Fault-sandbody coupling" accumulation model in the western Weak Compression Zone.

(3) Four key exploration directions for the next stage in the Central Anticline Belt of the Xihu Sag have been clarified: The preferred direction should be the large anticline structures in the northern medium-strong compression zone, which have superior reservoir-forming conditions and the potential to form large gas fields. In the strongly compressed anticlines, the EW-trending faults in the anticline cores should be avoided, and favorable lithologic traps should be sought in the flanks of the anticlines. In the weakly compressed zone, main oil and gas migration faults and their configuration relationship with sand bodies should be focused on and we should try to identify effective traps. For the deep ultra-low permeability field, gas reservoirs with high gas saturation should be sought around the areas developed under the paleo-structural background.

Author Contributions: Software, J.Q. and Z.Z.; Validation, Y.J.; Investigation, W.C., Z.X., F.J. and R.Z.; Writing—original draft, Y.C.; Supervision, Y.J. All authors have read and agreed to the published version of the manuscript.

Funding: This study was funded by the project named as Research on Exploration Direction and Key Technologies of Large Gas Fields of the Xihu Sag, East China Sea Shelf Basin (KJZX-2023-0101).

Institutional Review Board Statement: Not applicable.

Informed Consent Statement: Not applicable.

Data Availability Statement: The original contributions presented in the study are included in the article, further inquiries can be directed to the corresponding author.

Conflicts of Interest: Authors Yinshan Chang, Yiming Jiang, Jun Qin, Wenqi Chang, Zhiwu Xiong, Fujia Ji, Ruoyu Zhang were employed by Shanghai Branch of the China National Offshore Oil Corporation. The remaining authors declare that the re-search was conducted in the absence of any commercial or financial relationships that could be construed as a potential conflict of interest.

References

1. Zhou, X. Preface for the special issue of Xihu Depression in the East China Sea Shelf Basin. *Bull. Geol. Sci. Technol.* **2020**, *39*, 5. (In Chinese)
2. Zhou, X. Geological understanding and innovation in Xihu sag and breakthroughs in oil and gas exploration. *China Offshore Oil Gas* **2020**, *32*, 1–12. (In Chinese with English Abstract)
3. Zhang, Y.; Hu, S.; Liu, J.; Chen, Z.; Jiang, Y.; Zou, W.; Diao, H. Gas accumulation conditions and mode in X sag of East China Sea Basin. *China Offshore Oil Gas* **2022**, *34*, 27–35. (In Chinese with English Abstract)
4. Zhang, Y.; Hu, S.; Chen, Z.; Cai, H.; Jiang, Y.; Diao, H.; Wang, C. The genesis, accumulation model and exploration significance of Y gas field in X Sag, East China Sea Basin. *Haiyang Xuebao* **2022**, *44*, 88–98. (In Chinese with English Abstract)
5. Zhang, Y.; Zou, W.; Chen, Z.; Jiang, Y.; Diao, H. The mechanism of 'convergence ahead of accumulation' and its geological significance for gas reservoirs in Paleogene Huagang Formation across the central inverted structural zone of Xihu Depression, East China Sea Shelf Basin. *Oil Gas Geol.* **2023**, *44*, 1256–1269. (In Chinese with English Abstract)
6. Liu, J.; Zhang, S. Natural gas migration and accumulation patterns in the central-north Xihu Sag, East China Sea Basin. *Nat. Gas Geosci.* **2021**, *32*, 1163–1176. (In Chinese with English Abstract)
7. Gao, W. Major controlling factors and enrichment rules of highly efficient gas reservoiring in the north-central part of the central inversion belt, Xihu Depression. *Bull. Geol. Sci. Technol.* **2020**, *39*, 40–48. (In Chinese with English Abstract)
8. Yang, Y.; Huang, Z.; Qu, T.; Li, Z.; Wang, R.; Zhang, J.; Ma, C.; Pan, Y.; Yu, J. Main controlling factors and reservoir forming models of oil and gas reservoirs in Huangyan area, Xihu Sag, East China Sea Basin. *Geol. Rev.* **2023**, *69*, 2179–2194. (In Chinese with English Abstract)
9. Ken, E.P.; Martin, G.F. Applications of petroleum geochemistry to exploration and reservoir management. *Org. Geochem.* **2002**, *33*, 5–36.
10. Sharaf, L.M. Source rock evaluation and geochemistry of condensates and natural gases, offshore Nile Delta, Egypt. *J. Pet. Geol.* **2006**, *26*, 189–209. [CrossRef]
11. Arouri, K.R.; Laer, P.J.V.; Prudden, M.H.; Jenden, P.D.; Carrigan, W.J.; Al-Hajji, A. Controls on hydrocarbon properties in a Paleozoic petroleum system in Saudi Arabia: Exploration and development implications. *Aapg Bull.* **2010**, *94*, 163–188. [CrossRef]
12. Bloch, S.; Lander, R.H.; Bonnell, L. Anomalously high porosity and permeability in deeply buried sandstone reservoirs: Origin and predictability. *AAPG Bull.* **2002**, *86*, 301–328.
13. Ramm, M.; Bjorlykke, K. Porosity/depth trends in reservoir sandstones; assessing the quantitative effects of varying porepressure, temperature history and mineralogy, Norwegian Shelf data. *Clay Miner.* **1994**, *29*, 475–490. [CrossRef]
14. Xu, Z.; Yue, D.; Wu, S.; Zhang, X.; Chen, C.; Ni, Y. An analysis of the types and distribution characteristics of natural gas reservoirs in China. *Pet. Sci.* **2009**, *6*, 38–42. [CrossRef]
15. Hooper, E.C.D. Fluid migration along growth faults in compacting sediments. *J. Pet. Geol.* **1991**, *14*, 161–180. [CrossRef]
16. Hindle, A.D. Petroleum Migration Pathways and Charge Concentration: A Three-Dimensional Model. *AAPG Bull.* **1997**, *81*, 1451–1481.
17. Aydin, A. Fractures, faults, and hydrocarbon entrapment, migration and flow. *Mar. Pet. Geol.* **2000**, *17*, 797–814. [CrossRef]
18. Boles, J.R.; Eichhubl, P.; Garven, G.; Jim, C. Evolution of a hydrocarbon migration pathway along basin-bounding faults: Evidence from fault cement. *AAPG Bull.* **2004**, *88*, 947–970. [CrossRef]
19. Allan, U.S. Model for hydrocarbon migration and entrapment within faulted structures. *Aapg Bull.* **1989**, *70*, 803–811.
20. Gartrell, A.; Zhang, Y.; Lisk, M.; David, D. Fault intersections as critical hydrocarbon leakage zones: Integrated field study and numerical modelling of an example from the Timor Sea, Australia. *Mar. Pet. Geol.* **2004**, *21*, 1165–1179. [CrossRef]
21. Wang, Y.; Chen, J.; Pang, X.; Wang, G.; Hu, T.; Zhang, B.; Huo, Z.; Chen, H. Hydrocarbon migration along fault intersection zone—A case study on Ordovician carbonate reservoirs in Tazhong area, Tarim Basin, NW China. *Geol. J.* **2016**, *52*, 832–850. [CrossRef]
22. Ostanin, I.; Anka, Z.; Primio, R. Role of Faults in Hydrocarbon Leakage in the Hammerfest Basin, SW Barents Sea: Insights from Seismic Data and Numerical Modelling. *Geosciences* **2017**, *7*, 28. [CrossRef]
23. Liu, J.; Xu, H.; Jiang, Y.; Wang, J.; He, X. Mesozoic and Cenozoic basin structure and tectonic evolution in the East China Sea Basin. *Acta Geol. Sin.* **2020**, *94*, 675–691. (In Chinese with English Abstract)

24. Zhang, G.; Zhang, J. A discussion on the tectonic inversion and its genetic mechanism in the East China Sea Shelf Basin. *Earth Sci. Front.* **2015**, *22*, 260–270. (In Chinese with English Abstract)
25. Yang, F.; Xu, X.; Zhao, W.; Sun, Z. Petroleum accumulations and inversion structures in the Xihu Depression, East China Sea Basin. *J. Pet. Geol.* **2011**, *34*, 429–440. [CrossRef]
26. Wang, Q.; Li, S.; Guo, L.; Suo, Y.; Dai, L. Analogue modelling and mechanism of tectonic inversion of the Xihu Sag, East China Sea Shelf Basin. *J. Asian Earth Sci.* **2017**, *139*, 129–141. [CrossRef]
27. Zhu, W.; Zhong, K.; Fu, X. The formation and evolution of the East China Sea Shelf Basin: A new view. *Earth-Sci. Rev.* **2019**, *190*, 89–111.
28. Gu, H.; Jia, J.; Ye, J. Characteristics of oil and gas bearing system in Xihu lake depression in the East China Sea. *Oil Gas Geol.* **2002**, *23*, 295–297. (In Chinese with English Abstract)
29. Xu, X.; Chen, L.; Wang, Q. Analysis of Mesozoic Geological Characteristics and Resource Potential in the East China Sea Shelf Basin. *Mar. Pet.* **2004**, *24*, 1–7. (In Chinese with English Abstract)
30. Eadington, P.J.; Lisk, M.; Krieger, F.W. Identifying Oil Well Sites. U.S. Patent No. 5543616, 6 August 1996.
31. Lisk, M.; O'Brien, G.W.; Eadington, P.J. Quantitative Evaluation of the Oil-Leg Potential in the Oliver Gas Field, Timor Sea, Australia. *AAPG Bull.* **2002**, *86*, 1531–1542.
32. Wang, F.; Shi, Y.; Zeng, H.; Liu, K. To Identify Paleo-Oil Reservoir and to Constrain Petroleum Charging Model Using the Abundance of Oil Inclusions. *Bull. Mineral. Petrol. Geochem.* **2006**, *25*, 12–18. (In Chinese with English Abstract)
33. Chen, J. The Characteristics of Inclusions of Northeast Sichuan Fossil Oil Reservoir and Its Significance. Master's Thesis, Chengdu University of Technology, Chengdu, China, 2013. (In Chinese with English Abstract)
34. Lisk, M.; George, S.C.; Summons, R.E. Mapping hydrocarbon charge histories: Detailed characterisation of the South Pepper Oil Field, Carnarvon Basin. *Appea J.* **1996**, *36*, 445–464. [CrossRef]
35. Shen, Y.; Jia, D.; Song, G.; Ding, X.; Li, M. Reservoir-forming characteristics, key control factors and geological evaluation in the area outside oil source. *Geol. Rev.* **2010**, *56*, 51–59. (In Chinese with English Abstract)
36. Li, W.; Yi, H.; Hu, W.; Yang, G.; Xiong, X. Tectonic evolution of Caledonian paleohigh in the Sichuan Basin and its relationship with hydrocarbon accumulation. *Nat. Gas Ind.* **2014**, *34*, 8–15. (In Chinese with English Abstract)
37. Sun, W.; Liu, S.; Han, K.; Mise, Z.; Dai, H.; Sun, D. Effect of the evolution of paleotectonics on the petroleum genesis in Yanshan period, Sichuan Basin, China. *J. Chengdu Univ. Technol.* **2012**, *39*, 70–75. (In Chinese with English Abstract)
38. Ma, W.; Wei, Y.; Li, X.; Tao, S.; Li, Y.; Zhao, Z. Accumulation Process and Control Factors of Jurassic-Cretaceous Distant-Source and Secondary-Filled Reservoirs in the Hinterland of Junggar Basin. *Acta Sci. Naturlium Univ. Pekin.* **2018**, *54*, 1195–1204. (In Chinese with English Abstract)
39. Zhou, X. Oil and gas Pool-forming process and tectonic evolution of Cenozoic in Kuqa Petroleum system of Tarim Basin. *J. Palaeogeogr.* **2002**, *4*, 75–82. (In Chinese with English Abstract)
40. Zhang, Y. Petroleum geology and hydrocarbon distribution pattern of Huagang Formation in the Xihu Sag of the East China Sea. *Pet. Geol. Exp.* **2010**, *32*, 223–226. (In Chinese with English Abstract)